

# On the improvement of NO<sub>2</sub> satellite retrievals – aerosol impact on the airmass factors

J. Leitão<sup>1</sup>, A. Richter<sup>1</sup>, M. Vrekoussis<sup>1</sup>, A. Kokhanovsky<sup>1</sup>, Q. J. Zhang<sup>2</sup>, M. Beekmann<sup>2</sup>, and J. P. Burrows<sup>1</sup>

<sup>1</sup>Institute of Environmental Physics, University of Bremen, Bremen, Germany

<sup>2</sup>Laboratoire Inter-Universitaire des Systèmes Atmosphériques (LISA), CNRS et Universités Paris 12 et Paris 7, Créteil, France

Received: 18 November 2009 – Published in Atmos. Meas. Tech. Discuss.: 11 December 2009

Revised: 30 March 2010 – Accepted: 31 March 2010 – Published: 16 April 2010

**Abstract.** The accurate determination of nitrogen dioxide (NO<sub>2</sub>) tropospheric vertical columns from satellite measurements depends strongly on the airmass factor (AMF) used. A sensitivity study was performed with the radiative transfer model SCITRAN to better understand the impact of aerosols on the calculation of NO<sub>2</sub> AMFs. This influence was studied by varying the NO<sub>2</sub> and aerosol vertical distributions, as well as physical and optical properties of the particles. In terms of aerosol definitions, the key factors for these calculations were identified as the relation between trace gas and aerosol vertical profiles, the optical depth of the aerosol layer, and single scattering albedo. In addition, surface albedo also has a large impact on the calculations. Overall it was found that particles mixed with the trace gas increases the measurements' sensitivity, but only when the aerosol is not very absorbing. The largest change, a factor of ∼2 relative to the situation without aerosols, was found when a low layer of aerosol (600 m) was combined with a homogeneous NO<sub>2</sub> layer of 1.0 km. A layer of aerosol above the NO<sub>2</sub> usually reduces the sensitivity of the satellite measurement. This situation is found mostly for runs with discrete elevated aerosol layers (representative for long-range transport) that can generate a decrease of the AMF values of up to 70%. The use of measured aerosol profiles and modelled NO<sub>2</sub> resulted, generally, in much smaller changes of AMF relative to the pure Rayleigh case. Exceptions are some events of elevated layers with high aerosol optical depth that lead to a strong decrease of the AMF values. These results highlight the importance of aerosols in the retrieval of tropospheric NO<sub>2</sub> columns from space and indicate the need for detailed information on aerosol properties and vertical distribution.

## 1 Introduction

The possibility of measuring trace gases (e.g. ozone (O<sub>3</sub>), nitrogen dioxide (NO<sub>2</sub>), sulphur dioxide (SO<sub>2</sub>), among others) from space provides a unique opportunity to observe the Earth and its atmosphere from above and, consequently, monitor the air quality in remote places with low density of in situ measurements. Remote sensing of atmospheric pollution is currently performed by several instruments flying on satellites. One common technique is the use of backscattered solar radiation from which information can be retrieved on the amounts of aerosols and trace gases in the atmosphere. Some instruments were mainly developed for trace gas observations, as it is the case for GOME (Burrows et al., 1999) flying on ERS-2, SCIAMACHY (Burrows et al., 1995; Bovensmann et al., 1999) on the ENVISAT platform, OMI (Levelt et al., 2006) on EOS-AURA and more recently GOME-2 (Calliches et al., 2000) launched on MetOp-A. These also provide information on aerosols (mainly aerosol optical depth (AOD) but also, e.g., aerosol size distribution) albeit at low spatial resolution. Other instruments such as MODIS (King et al., 1992) flying on Terra and Aqua, MISR (Diner et al., 1998) also on Terra measuring with multi-angle viewing directions, or MERIS (Bézy et al., 2000) on the ENVISAT platform, are better suited for aerosol retrievals since they provide high spatial resolution and, in some cases, multiple viewing directions. More recently, the active lidar system CALIOP (Winker et al., 2003) flying on the CALIPSO satellite has become available which for the first time can resolve aerosol vertical distributions with high resolution.

Nitrogen oxides (NO<sub>x</sub>=NO+NO<sub>2</sub>) can be considered one of the main pollutants present in urban and industrialized areas, originating mainly from fossil fuel combustion processes. NO<sub>x</sub> is also emitted from biomass burning events and via natural processes mostly during lightning events and as result of microbial processes in soils. NO<sub>x</sub> play a key role in the basic tropospheric chemistry acting as a precursor



Correspondence to: J. Leitão  
(jleitao@iup.physik.uni-bremen.de)

for photochemical ozone production and acidification of the atmosphere via nitric acid (Seinfeld and Pandis, 1998). Furthermore, they also contribute to global climate change by interfering, directly and indirectly, with the Earth's radiative budget (Solomon et al., 1999; IPCC, 2007; Vasilkov et al., 2009). According to the recent Fourth Assessment Report (AR4, IPCC, 2007 and references therein), anthropogenic NO<sub>x</sub> emissions have increased drastically since preindustrial times. While emissions in some industrialized countries have decreased over the last decade in response to emission reduction measures and use of cleaner fuels, emissions in the rapidly developing economies in Asia are expected to continue their increase. In the mid-1990s NO<sub>x</sub> emission rates for Asia were reported by Akimoto (2003) to exceed the amount emitted in North America and Europe, and in 2005, Richter et al. found a high enhancement of NO<sub>2</sub> columns over China measured by GOME and SCIAMACHY. While the global budget of anthropogenic sources is relatively well constrained, the natural emissions are still rather uncertain. Ground-based measurements and model studies aim on assessing pollution levels and analyse evolution trends. To estimate accurate NO<sub>2</sub> concentrations, the satellite datasets offer advantages both on the time and spatial scales with a nearly global coverage that can often be achieved with high temporal resolution (approx. 1 to 6 days depending on the instrument coverage).

Although a great fraction of aerosols is part of the natural components of the Earth's atmosphere, they can still be harmful for human health and contribute to visibility degradation when present in high amounts (Chang et al., 2009 and references therein; Wang et al., 2009). In addition to their relevance as pollutants, they play a major role in climate change by their direct and indirect impact on radiative forcing (e.g. IPCC, 2007). Aerosols vary strongly in size and composition, and their proper characterization, in particular using remote sensing, is still a challenge. In recent years numerous experimental studies focused on aerosols. Still, the formation processes, transport and transformation of aerosols are not completely understood. Their high spatial and temporal variability (especially for tropospheric aerosol) represents a complication to the process of identifying and quantifying its sources and types.

Aerosol present in the atmosphere interacts with radiation consequently influencing the remote sensing measurements of atmospheric trace gases. Depending on the particles' optical properties, the amount of aerosol and its vertical distribution relative to that of the trace gas of interest, the sensitivity of the satellite measurements can either be increased or decreased. As the anthropogenic sources of aerosols and other pollutants are often collocated, a proper characterization of the aerosols' impact on the retrieval is needed to accurately quantify trace gas amounts derived from satellite observations. This is of particular importance if long-term trends of, for example, tropospheric NO<sub>2</sub> are studied which are accompanied by large changes also in the aerosol loading.

Several aspects contributing to the total error in the determination of tropospheric NO<sub>2</sub> columns from the satellite measurements were studied by Boersma et al. (2004). In that analysis it was reported that including realistic aerosol in the radiative transfer calculations would increase the airmass factors by up to 40% depending on aerosol type and aerosol optical depth. The vertical profile of the aerosols was assumed to be exponential with a scale height of 2.0 km and the vertical NO<sub>2</sub> profile was not specified. The conclusion from this study was that the correction for the aerosol impact cannot be simply separated from the effect of clouds and, therefore, if a cloud retrieval scheme is adopted, it will account for a large part of the aerosol effect by retrieving a different cloud fraction and height. Martin et al. (2003) also analysed the aerosol impact on the airmass factor applied in the retrieval process. Monthly aerosol properties derived with the GOCART model were used for that study. The authors found that biomass burning aerosol and desert dust would reduce the AMF by 10–20% while over industrial regions an increase of 5–10% was observed.

A comparable sensitivity study to the one presented here was carried out by Gloudemans et al. (2008) to analyse, among other aspects, the impact of aerosols in the retrieval of CH<sub>4</sub> and CO (in the IR region) from the SCIAMACHY instrument. One of the main findings from this study was that, depending on the location of the plume and type of aerosol, the omission of aerosol influence in the retrieval process can lead to significant errors in the total column of CH<sub>4</sub>. Thomas et al. (2005), with a similar study for SO<sub>2</sub> (retrieved in the UV region) concluded that aerosols are relevant mainly for optical thickness above 0.3 and in the presence of desert dust plumes in the boundary layer (BL). If these two conditions were realised at the same time the authors estimated that the column would be underestimated by 5–10%. For the TOMS SO<sub>2</sub> retrieval, Krueger et al. (1995) showed that neglecting a rather thin aerosol layer may result in a systematic overestimation of the retrieved total SO<sub>2</sub> content. Focusing on HCHO retrieval, Fu et al. (2007) have also analysed the sensitivity of the AMF to aerosol definitions. From the results, the relative vertical distribution of the trace gas and aerosol was identified as major factor influencing the AMF. A strong enhancement of the AMF was observed for the case of an aerosol layer standing below the HCHO.

Furthermore, recently, the aerosol impact on ground-based zenith-sky DOAS measurements was also investigated by Chen et al. (2009). The aerosol effect was studied by changing the vertical distribution of aerosol and NO<sub>2</sub> layers, together and independently of each other, and varying also the single scattering albedo (SSA). From this analysis an error of 10% was determined. Nevertheless, for these measurements, the uncertainties caused by unknown aerosol properties and vertical profiles of both aerosol and NO<sub>2</sub> tended to cancel each other.

The present study assesses the importance of aerosol for the retrieval of tropospheric NO<sub>2</sub> columns from satellite observations in clear sky cases. The effects of clouds in the retrieval were already analysed in detail in many previous studies such as Boersma et al. (2004), Wang et al. (2005) and Kokhanovsky and Rozanov (2009). Therefore, this study focussed mainly on the aerosol effect and, to this end, a number of different scenarios were defined with varying aerosol settings and NO<sub>2</sub> distributions. Those were used for radiative transfer calculations with the SCIASTRAN model (Rozanov et al., 2005) in order to evaluate changes in the measurements' sensitivity relative to a scenario without aerosols. The results show to which parameters the measurements are most sensitive and to which extent the modification of aerosol properties affects the results. As far we are aware, a comprehensive study as ours has not been conducted before. In this analysis the impact of clouds was not taken into account in the calculations but will be discussed briefly after the main results.

The paper starts with an introduction of aerosol effects on radiative transfer and a short description of the satellite retrieval and the AMF concept. In addition, a description is provided for the selection process of data used and definition of the case scenarios considered. The following section focuses on the results of the sensitivity study, presenting the variations of NO<sub>2</sub> airmass factors in response to changes in the surface albedo values, the boundary layer height, variation in the aerosol layer distribution and use of different single scattering albedo values. A discussion on the possible cloud effects and current algorithms is presented in Sect. 5, followed by general conclusions in the final section of this manuscript.

## 2 Methodology

### 2.1 The effect of aerosols on the radiative transfer

Satellite measurements of tropospheric trace gases using scattered solar light are based on detection of the absorption along the light path from the sun through the atmosphere to the instrument. For an ensemble of photons, scattering is regarded as a statistical process, where many different light paths contribute to the signal observed at the top of the atmosphere. For an optically thin absorber, the overall absorption signal is determined by the amount of absorption along the individual light paths weighted with their relative contributions to the total radiance measured. In comparison to a pure Rayleigh atmosphere, the presence of aerosols can change both the individual light path lengths and their contributions to total radiance observed at the satellite.

Qualitatively, the effects of an aerosol layer on tropospheric measurements using scattered sun light can be separated into four groups:

- light path enhancement within the aerosol layer as result of multiple scattering, leading to an increase in absorption signal from the path between scattering events;
- increased sensitivity within and above the aerosol layer as result of larger scattering probability and therefore a larger contributions of these paths to the radiance observed at the satellite (albedo effect);
- decreased sensitivity below the aerosol layer as more photons are scattered back to the satellite before they can reach these altitudes (shielding effect);
- decreased sensitivity within and below the aerosol layer in cases of strongly absorbing aerosols as the number of photons returning from this region is reduced.

With the exception of the last point, the effects of aerosols listed above are very similar to the considerations made for clouds (e.g. Hild et al., 2002; Beirle et al., 2009; Kokhanovsky and Rozanov, 2009). The overall impact of aerosols on a measurement will depend on the relative importance of the above mentioned effects which depends mainly on aerosol properties, aerosol amounts, surface reflectance and the vertical distribution of aerosol and trace gas of interest, but also on the solar zenith angle (SZA) and satellite viewing angle. The results can be both, an increase or a decrease in observed absorption signal depending on the specific conditions.

### 2.2 The AMF

One way of expressing the sensitivity of the measurement is to calculate the airmass factor (AMF) which is defined as the ratio between the apparent (slant) column (SC) of the absorber retrieved from a measurement and the vertical atmospheric column (VC, Solomon et al., 1987):

$$\text{AMF} = \text{SC} / \text{VC}. \quad (1)$$

The definition can be generalised by applying it to discrete layers in different altitudes, defining the block airmass factor (BAMF) for a layer  $i$ :

$$\text{BAMF}_{(i)} = \frac{\text{SC}_{(i)}}{\text{VC}_{(i)}}, \quad (2)$$

which describes the change of airmass factor with altitude. The AMF can be computed from the BAMF by weighting it with the atmospheric absorber profile:

$$\text{AMF} = \frac{\sum_i^N (\text{BAMF}_{(i)} \cdot \text{VC}_{(i)})}{\sum_i^N \text{VC}_{(i)}}, \quad (3)$$

where  $\text{VC}_{(i)}$  is the vertical column of the absorber in layer  $i$  and  $N$  is the total number of layers. More detailed discussions of the airmass factor concept can be found in Wagner et al. (2007) and Rozanov and Rozanov (2010).

The larger the airmass factor, the higher the sensitivity of the measurement. The aerosol effects discussed in the previous section are illustrated in Fig. 1 where the NO<sub>2</sub> block airmass factor is shown as function of altitude for three different scenarios, highlighting the increased sensitivity in the presence of aerosols in the upper part of the layer and above it as well as the reduced sensitivity close to the surface.

The AMF is computed using radiative transfer calculations that require information on measurement conditions (such as, observation geometry and wavelength) and atmospheric characteristics (e.g., vertical distribution of the chemical species, surface albedo, aerosol loading and clouds). Hence, an appropriate selection of the a priori assumptions used is essential to obtain the correct values of the AMF and thus reduce the uncertainties of the NO<sub>2</sub> columns. Selecting an AMF that is too high will result in an underestimation of the VC. Likewise, the determined NO<sub>2</sub> VC will be too large if the value of the AMF used for the conversion of the SC is too small.

### 2.3 Satellite retrieval

The retrieval of tropospheric NO<sub>2</sub> columns from space is performed in several steps. First, NO<sub>2</sub> slant column densities (SC) are retrieved with the DOAS (Differential Optical Absorption Spectroscopy) technique (Platt and Stutz, 2008) in the UV/visible wavelength range. The SC corresponds to the amount of absorber present along the average light path through the atmosphere to the satellite sensor. The tropospheric SC is calculated by eliminating the stratospheric contribution from the total columns retrieved (further details regarding the retrieval can be found, for example in Leue et al. (2001), Richter and Burrows (2002), Martin et al. (2002) and Boersma et al. (2004)). As explained above, when dividing this tropospheric SC by an appropriate airmass factor a NO<sub>2</sub> tropospheric vertical column is obtained.

In current retrieval methods the presence of aerosols in the atmosphere is included in many different ways. Some retrieval processes do not explicitly correct for aerosol impact, arguing that the cloud correction scheme also accounts for a large part of the aerosol effect (Boersma et al., 2004, 2007). Another approach is to use a static a priori profile for aerosol loading and type (Nüß, 2005; Richter et al., 2005). Finally, some retrievals include full aerosol treatment in the radiative transfer using aerosol fields from models (Martin et al., 2003; Lee et al., 2009).

### 2.4 Radiative transfer settings

Numerous factors need to be accounted for when considering the effect of aerosols on satellite NO<sub>2</sub> measurements. In the present study, these effects were analysed in detail by considering multiple scenarios where the aerosol vertical distribution was varied together with its load and optical properties. In addition, as it will be explained below, the surface

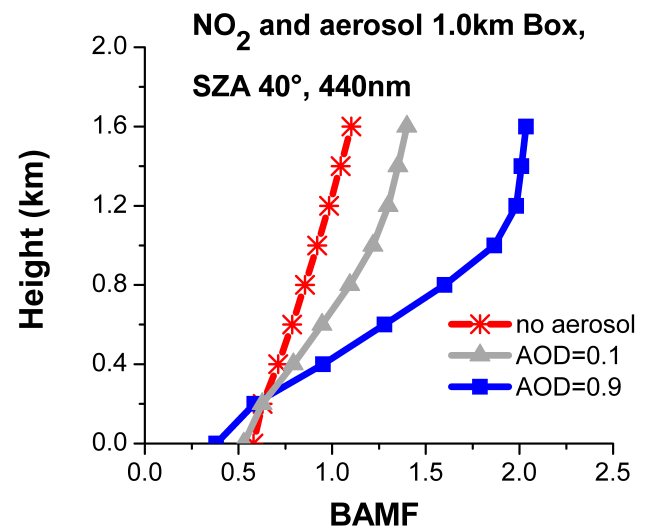


**Fig. 1.** NO<sub>2</sub> block airmass factor (BAMF) for 3 scenarios: no aerosol (red), and an aerosol layer with SSA of 0.93 extending from the surface to 1.0 km with an optical depth (AOD) of 0.1 (grey) and 0.9 (blue). AMFs determined at 440 nm, with surface albedo = 0.03,  $\omega_0 = 0.93$  and solar zenith angle (SZA) 40°.

albedo value and the NO<sub>2</sub> vertical profile were also varied. Airmass factors were calculated with the radiative transfer model SCIATRAN 2.2 (Rozanov et al., 2005). The calculations were performed on a vertical grid of 200 m from surface to the top of the trace gas and aerosol layers, at four different wavelengths (425, 437.5, 440 and 450 nm), in nadir observation, and at six solar zenith angles (SZA, from 20° to 70° in steps of 10°). SCIATRAN was operated using the discrete ordinate method for solution of the radiative transfer equation, in plane parallel geometry, accounting for full multiple scattering effects, but without including polarization. At the viewing geometry used here, the effects of Earth's curvature and refraction can be neglected. As atmospheric scenario, the US standard atmospheric pressure and temperature were used. The surface albedo was set to 0.03 assuming that this is, for the spectral range used, an average value for urban areas. Nevertheless, this value was also varied to 0.01, 0.07 and 0.1 so that the effect of the surface albedo on the calculations could be determined.

In a first step, simplified scenarios were investigated with, for example, NO<sub>2</sub> and aerosol vertical distribution as box profiles and considering purely scattering or partly absorbing aerosols. The results from these simulations provide insight into the direction and magnitude of the effects of different parameters on the satellite sensitivity. Furthermore, a second phase of the study included measured aerosol profiles from different locations and NO<sub>2</sub> profiles from model simulations for urban and rural conditions. In both cases, the interference exerted by aerosols can be analysed by comparing these scenarios with a reference scenario where no aerosol

is considered in the radiative transfer calculations. In following sections the scenario assumptions will be described in more detail and these settings are also summarized in Tables 1 and 2.

#### 2.4.1 NO<sub>2</sub> profile

For the initial analysis, the NO<sub>2</sub> profiles were considered to be homogeneously distributed within a boundary layer of 0.6, 1.0 or 2.0 km height (box profiles). This homogenous distribution is, most probably, not often found close to the major anthropogenic sources, i.e., in urban locations. For that reason, in other case scenarios simulated, two different NO<sub>2</sub> profiles, from surface to 5.5 km, were used: average urban and rural. These profiles are an average from CHIMERE (Schmidt et al., 2001; Honoré et al., 2008) model runs with a 9 × 9 km<sup>2</sup> resolution, at 10 LT and for the period from 23 May to 11 June 2007 (randomly selected). The NO<sub>2</sub> volume mixing ratio above 5.5 km (the top of model simulations) decreases slowly to a value of  $1.5 \times 10^{-6}$  ppm at 100 km. The model results are based on a simulation for Paris downtown, a location in the close vicinity of Paris at 15 km East and a rural region at 100 km East of Paris. Since the first two sites are very similar, and, considering that the typical size of a satellite pixel would include both of these measurements, their average is defined as average urban – “Avg Urb”. Near surface NO<sub>2</sub> levels in this profile are close to the climatological average of urban background surface NO<sub>2</sub> within in the Paris town and its near suburbs of above 20 ppb (<http://www.airparif.asso.fr/>). While the model does not consider lightning explicitly, NO<sub>x</sub> (background) from this source are included via the boundary conditions for the domain. In Fig. 2 the different NO<sub>2</sub> mixing ratio profiles are shown from surface up to 10 km. As it can be seen in the profiles presented in Fig. 2, the NO<sub>2</sub> profile determined by the model for the urban conditions is not at all similar to a homogenous distribution over a boundary layer of 1.0 km or even 600 m. This has a significant impact on the results as it will be further discussed in Sect. 3.3. In addition, the large difference between the urban and rural profiles illustrates how the NO<sub>2</sub> vertical distribution can show significant variations over a short distance. This might be a crucial point for satellite retrievals where, at the spatial resolution of current a priori data, both urban and rural scenes are often contained in one model grid cell (Heckel et al., 2010).

#### 2.4.2 Aerosol settings

Currently, several datasets of aerosol characteristics are available from records of either ground-based or satellite instruments (e.g. MODIS, MISR, MERIS, CALIPSO, etc.). Worldwide ground-based networks offer the possibility to obtain crucial information to better characterize aerosols and reduce the current uncertainties on the definition of aerosol optical properties. This is the case of, for instance, the

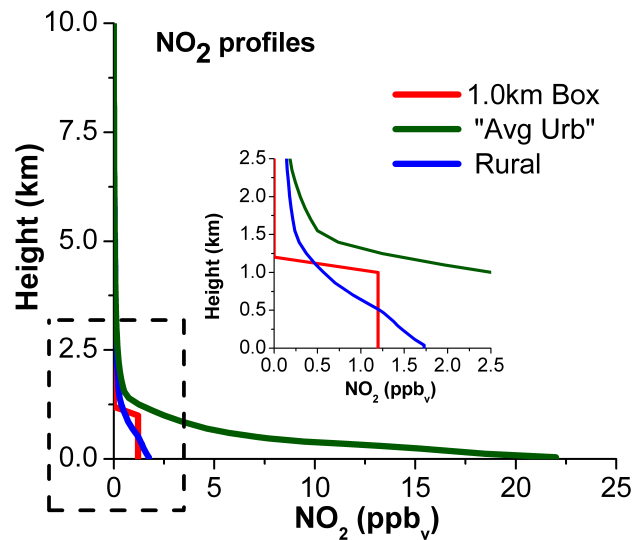


**Fig. 2.** NO<sub>2</sub> profiles from surface to 10.0 km used in the SCIA-TRAN settings for the airmass factor calculations: box profile of 1.0 km (red); average urban (“Avg Urb”, green) and rural (blue) based on CHIMERE model results.

Aerosol Robotic Network (AERONET, Holben et al., 1998), the European Aerosol Research Lidar Network (EARLINET, Mattis et al., 2002), or the Asian dust network (AD-net, Murayama et al., 2001). In the present study data from these networks was applied in the definition of the aerosol optical properties and its vertical distribution. The optical properties and size distributions, at 440 nm, were mainly taken from records of 12 worldwide AERONET stations presented in Dubovik et al. (2002). This dataset is representative for the usual classification of four different aerosol types that have distinctive physicochemical, optical and radiative properties: urban/industrial, biomass burning, desert dust and oceanic. The precision of the AERONET dataset is discussed in detail in several publications but this subject will not be explored here because the accuracy of these measurements and representativeness of the dataset is not central to the conclusions to be drawn.

#### Size distribution and phase function

Aerosols emitted in urban areas and from open vegetation fires are, on average, dominated by small particles (Seinfeld and Pandis, 1998). Yet, the size distribution of this aerosol, especially that of biomass burning cases, is not constant and varies in time and space. The dimension of the particles is mostly dependent on the type of fuel, the combustion phase and the age of smoke (e.g. Dubovik et al., 2002). This last factor can be important when considering fire plumes that are transported for some days away from the source. On the other hand, mostly coarse particles are found in desert dust

scenes or oceanic aerosol (Seinfeld and Pandis, 1998). The selection of results presented here will follow these assumptions, i.e., not every simulated case will be shown but mostly those which are more representative of the aerosol type in consideration. In order to facilitate the interpretation of results, a mixing of fine and coarse aerosol, as it would happen in reality, was not simulated.

Within the radiative transfer model, angular distributions of scattered light are required to simulate the interaction of particles and light. The details of the angular distribution of the phase function vary with the aerosol composition and the size of the particles relative to the wavelength of the radiation and also depend on particle shape and internal structure. For each of the aerosol types, the phase functions (see Fig. 3) for both fine and coarse particles were considered. These were determined with a FORTRAN program developed by Michael Mishchenko and freely available at <http://www.giss.nasa.gov/staff/m mishchenko/brf/>.

### Single scattering albedo

The scattering efficiency of aerosols strongly depends on their concentration, size and shape, as well as on their refractive index, determined by their chemical composition. Aerosol scattering also depends on the scattering angle and usually has a pronounced maximum for forward scattering. Likewise, the absorbing properties of aerosols are usually expressed via the single scattering albedo (SSA) which is defined as the ratio of scattering to extinction and depends on particle composition and wavelength. The SSA differs according to type and source of aerosol and, therefore, is in part dependent on the location of measurement (see, for example, Hu et al., 2007). For the majority of the scenarios considered in this analysis, the impact of aerosol absorption was simply investigated by comparing the AMF determined with runs where  $\omega_0$  was set to 0.93 (average from all the SSA values given at 440 nm in Dubovik et al., 2002) and others where  $\omega_0=1.0$ . This allowed determining the maximum effect in the results when reducing the absorbing ability of aerosol. Furthermore, when evaluating the impact of the SSA in the radiative transfer calculations, this parameter was also set to 0.8 and 0.95 (see Sect. 3.5). In the second stage of the analysis, when considering measurements of aerosol profiles, the  $\omega_0$  values required were either taken from the corresponding records or based on typical values available from other studies that focused specifically on each of the aerosol types.

### Vertical distribution

For remote sensing applications, the total amount of aerosols present in the atmosphere is often specified by an aerosol optical depth (AOD) which is the vertical integral of the extinction by aerosols from the top of the atmosphere to the ground. In the first phase of the study, the aerosol vertical distribution

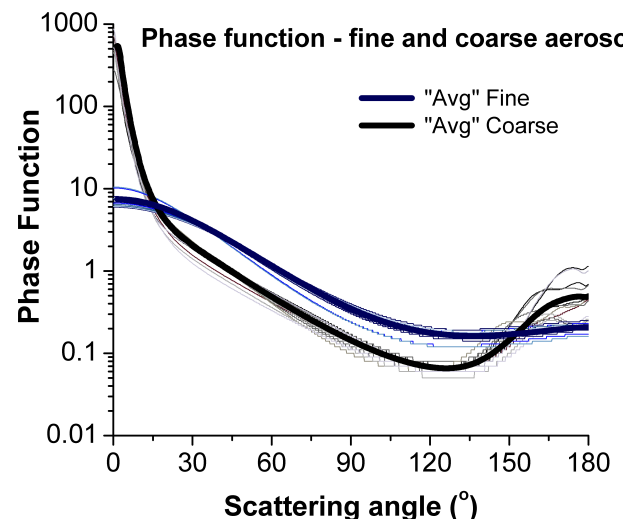


**Fig. 3.** Phase functions at 440 nm for fine (blue) and coarse (grey) aerosol determined for 4 distinct aerosol types: Urban (Urb), Biomass Burning (BB), Desert Dust (DD) and Oceanic. Optical properties taken from 12 AERONET stations (Dubovik et al., 2002): Paris/Creteil – France (Urb), GSFC/Maryland – USA (Urb), Maldives (Urb), Mexico city – Mexico (Urb), Amazonian Forest – Brazil (BB), South American cerrado – Brazil (BB), African savanna – Zambia (BB), Boreal forest – USA and Canada (BB), Cape Verde (DD), Persian Gulf (DD), Saudi Arabia (DD) and Lanai (Oceanic). Average of phase functions for each of the aerosol sizes considered is presented in thick lines (blue for fine and black for coarse aerosol).

was defined as a box shaped profile. These well defined layers with homogenously distributed aerosol had variable top height. Three cases were set with extinction coefficients representative for three aerosol loads: 0.1 (low pollution level), 0.5 (moderate pollution) and 0.9 (polluted scene) aerosol optical depths. Alternatively, the aerosol's vertical distribution was defined in different ways: following the NO<sub>2</sub> profile; starting at surface level and with the top of the layer lower or higher than that of the NO<sub>2</sub> profile; furthermore, discrete elevated aerosol layers above the NO<sub>2</sub> layer (assumed to be in the BL) were also taken into account. The scenarios A to H (Table 1) will probably not be realised for all types of aerosols. Normally, the urban aerosol is assumed to be either in homogenous layers extending from the surface to the top of BL or, often, following an exponential decrease with height. In general, one can assume that the majority of anthropogenic sources are the same for both NO<sub>2</sub> and aerosols and, therefore, they would have similar spatial distributions. However, depending on the source location and transport processes, the aerosol layer can extend to a higher altitude, whereas NO<sub>2</sub> will be in general more concentrated closer to the source region and at lower levels, due to a shorter life time. For that reason, the extension of each layer was also varied independently so that different scenarios could be

**Table 1.** Scenarios considered for the SCIATRAN runs, defined by the combination of a NO<sub>2</sub> and an aerosol layer, as in box profiles (e.g., Scenario B: NO<sub>2</sub> layer 0–1.0 km and aerosol layer 0–0.6 km).

Scenario	A	B	C	D	E	F	G	H
NO <sub>2</sub> layer (km)	0–0.6				0–1.0			0–2.0
Aerosol layer (km)	0–0.6	0–0.6	0–1.0	0.6–1.0	1.0–2.0	0–2.0	2.0–3.0	0–2.0

analysed. The scenarios with elevated discrete aerosol layers are mostly adequate to illustrate plumes of biomass burning smoke and desert dust that are transported several hundreds to thousand kilometres away from the source and which can be lifted to higher altitudes during transport. These events can happen not only on a continental scale (e.g. smoke from fires in the African savanna that is transported across the Atlantic Ocean) but also on a regional scale, like the transport within Europe. These aerosol plumes often occur in the free troposphere, but they can also be part of the boundary layer either by intrusion processes or due to the low initial injection height (Müller et al., 2003; Labonne et al., 2007). Good examples of this case are the dust outbreaks from deserts that often can mix with urban type aerosol emitted within European or Asian cities (e.g. Zhou et al., 2002).

In a second stage, the definition of the case studies was based on data available from different measurements. Like this, situations as those described above could be simulated. The size distribution and corresponding phase functions were maintained from the initial stage. Nevertheless, the extinction coefficients used for the profile definition were based on lidar measurements performed at numerous locations at different times of the year (see representation of profiles I to P in Fig. 4 and further details in Table 2). Still, the profiles considered in this study are not the exact representation of the original ones. Often adjustments were required in order to obtain a profile from surface to the top of atmosphere of 100 km. Moreover, as these are meant to be examples for case studies their accuracy is not a subject of this analysis and does not influence the conclusions drawn. Because lidar measurements (both satellite and ground-based) are usually performed at 355 nm and/or 532 nm an Ångström exponent (Ångström, 1929) was necessary to convert these values to the corresponding ones at 440 nm (within the wavelength region where NO<sub>2</sub> is retrieved). These values were also taken from the referred literature. The oceanic aerosol type was not included at this stage because this aerosol is normally only observed in very low concentrations at polluted sites and is usually mixed with other types of aerosol. Therefore, for simplicity of the analysis, it is assumed that its influence in the NO<sub>2</sub> retrieval is similar to that of the other types considered.

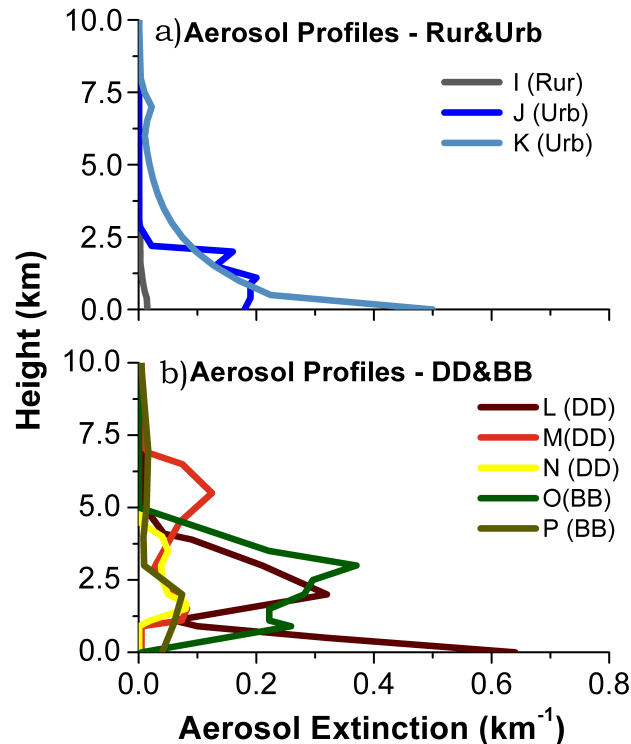


**Fig. 4.** Aerosol extinction profiles from surface level to 10.0 km used in the SCIATRAN settings for the airmass factor calculations for: (a) rural (Rur) and urban (Urb) locations; and (b) desert dust (DD) events and biomass burning (BB) plumes. These profiles are based on measurements performed at different locations as it is explained in Table 2.

### 3 Results

A comprehensive analysis was performed with airmass factors of NO<sub>2</sub> calculated for many different case studies where different settings of the model calculations were changed. Here only the results obtained for 440 nm are analysed as this is the wavelength for which the AERONET aerosol optical properties are given. Extension of the calculations to the wavelength range often used for NO<sub>2</sub> retrieval revealed an average increase of AMF by 10% from 425 to 450 nm. This variation is relatively small and will largely cancel if it is linear with wavelength but might be relevant in some cases. For different solar zenith angles (SZA), the general trend shows

**Table 2.** Aerosol parameters (single scattering albedo ( $\omega_0$ ), Ångström exponent ( $\alpha$ ) and aerosol optical depth, AOD) that were used to define the aerosol vertical profile (with extinction coefficients) for the SCIATRAN scenarios – taken from each of the references mentioned. These are representative of different aerosol types: Urban (Urb), Desert Dust (DD), and biomass burning (BB) scenes.

Scenario and Reference for aerosol ext. profile		Aerosol type	$\omega_0$	$\alpha$	AOD	Further notes
I	based on CALIPSO records <sup>a</sup>	Urb	0.93 <sup>b</sup>	1.4 <sup>c</sup>	0.07	Background conditions
J	Chazette et al. (2005)	Urb	0.87	2.1	0.40	19 July 2000 in Paris (FR)
K	Amiridis et al. (2005)	Urb	0.93 <sup>b</sup>	1.4 <sup>c</sup>	0.62	4 yr average over Thessaloniki (GR)
L	Zhou et al. (2002)	DD	0.92 <sup>b</sup>	0.19	1.05	12 May 2000 in Heifei (CN)
M	Murayama et al. (2003)	DD	Altitude dependent values – 0.8 to 0.95	Altitude dependent values – 0.01 to 1.1	0.66	23 April 2001 in Tokyo (JP)
N	Pérez et al. (2006)	DD	0.93	0.19 <sup>d</sup>	0.16	18 June 2003 in Barcelona (SP)
O	Balis et al. (2003)	BB	0.92 <sup>b</sup>	1.4 <sup>e</sup>	1.05	9 August 2001 in Thessaloniki (GR)
P	Müller et al. (2005)	BB	0.92 <sup>b</sup>	Altitude dependent values – 0 to 1.1	0.42	26 June 2003 in Leipzig (DE)

<sup>a</sup> Data provided by Chieko Kittaka and David Winker from NASA – Goddard Space Flight Center.

<sup>b</sup> Average of the respective aerosol type based on Dubovik et al. (2002).

<sup>c</sup> Average for urban aerosol in Mattis et al. (2004).

<sup>d</sup> Same as Zhou et al. (2002).

<sup>e</sup> From Müller et al. (2005) and references therein.

that the AMF increases for higher sun, but for specific cases, this tendency can also be reverted. In some circumstances (not presented here), when considering fine aerosol, a decrease occurs with high sun, and in other cases, with coarse particles, a small increase is then followed by decay after 50° or 60°. The variation of the size parameters (mean radius and its standard deviation within the fine or coarse mode categories) of the different aerosol types representative for the locations considered in this study was rather small. The similarity in values resulted in nearly identical phase functions with noticeable differences only between the two general size distributions considered: fine and coarse (see Fig. 3). As a result, the NO<sub>2</sub> AMF determined within the various scenarios with fine particles are very similar, and the same occurs for those with coarse aerosol. When comparing to the scenario without aerosol it was found that fine particles have a higher impact on intensifying the changes on the AMF than the coarse ones. However, this effect depends on many fac-

tors such as the vertical distribution or sun position (e.g., very low sun can favour the enhancement of signal by the coarse particles standing in a discrete layer above the trace gas). As expected the values of AMF determined with non-absorbing aerosol were the highest. This decrease in the measurements' sensitivity for absorbing aerosol is a consequence of the reduction of available light when such aerosol is present in the atmosphere. It is also important to note that at 440 nm the Rayleigh optical thickness is 0.32. Consequently, in scenarios I and N, the molecular scattering dominates.

### 3.1 Surface Albedo

The surface albedo selected for all scenarios included in this sensitivity study was 0.03. NO<sub>2</sub> is not measured only over urban areas but also in remote locations where the surface albedo can vary according to the different type of soil and vegetation. Knowing that the surface reflectivity is influencing the sensitivity of the satellite measurements, the impact

of changes in surface albedo was also analysed here. As mentioned above, this value was set to 0.01, 0.07 and 0.1 in a scenario of NO<sub>2</sub> and aerosol homogenously mixed in a 1.0 km layer (scenario C).

From the results presented in Fig. 5 it is possible to see that the impact of the surface albedo can be quite high in the AMF calculations. An increase of the surface albedo value results always in an increase of the AMF. Brighter surfaces will more efficiently reflect the sun light back to the satellite and therefore contribute to the enhancement of the measured NO<sub>2</sub> columns. A change from 0.01 to 0.1 can result in an increase of the AMF on average of 90% (for different AODs). The maximum value obtained is in fact much higher and changes by a factor of 2.8 are registered for the case of high sun (SZA of 20° and 30°), with coarse particles mixed with the trace gas and AOD=0.1. The dependence of this change on the aerosol amount present in the atmosphere is illustrated in panel (b) of Fig. 5 where the AMFs are plotted as a function of surface albedo, for one SZA (50°) and different AODs. The impact of aerosols is largest over dark surfaces and rapidly decreases as albedo increases as the increase in reflectivity resulting from aerosols has less effect if the surface is already bright. However, the situation changes when considering absorbing aerosol (results not shown). In that case, a decrease of the AMF is observed when a dark layer of aerosol (mixed with the trace gas) stands above a bright surface, i.e., surface albedo of 0.1 and above.

### 3.2 Changes in boundary layer height

The height of the boundary layer differs for different locations and is also dependent on seasonal variations. To investigate the effect of BL height changes alone, a study was carried out varying this height to 0.6, 1.0 and 2.0 km (scenarios A, C and H, respectively), and maintaining both the NO<sub>2</sub> and aerosol homogenously distributed in this layer. In Fig. 6 the results obtained for urban fine and coarse aerosol with different aerosol optical thickness are presented.

Before discussing the impact of the boundary layer height with trace gas and aerosol mixed in the atmosphere it is important to mention that the variations of the boundary layer influence the AMF calculations even when considering only a layer of NO<sub>2</sub> without aerosol present. When the top of the NO<sub>2</sub> layer expands from 0.6 to 2.0 km the AMF will increase in average by a factor of 1.4. This is related to the fact that the sensitivity of the measurements is smaller close to the surface. For every case (from scenarios A, C and H) it was found that the smallest AMFs are determined for the conditions without aerosol (not shown). Thus, one can conclude that, in these scenarios, the presence of aerosol results in an increase of the sensitivity of the measurements, even if quite small for coarse particles and low aerosol load. In practice, this indicates that, for the cases exemplified here, if the effect of aerosol scattering is not accounted for in the retrieval, the NO<sub>2</sub> VC will be overestimated. Furthermore, comparing

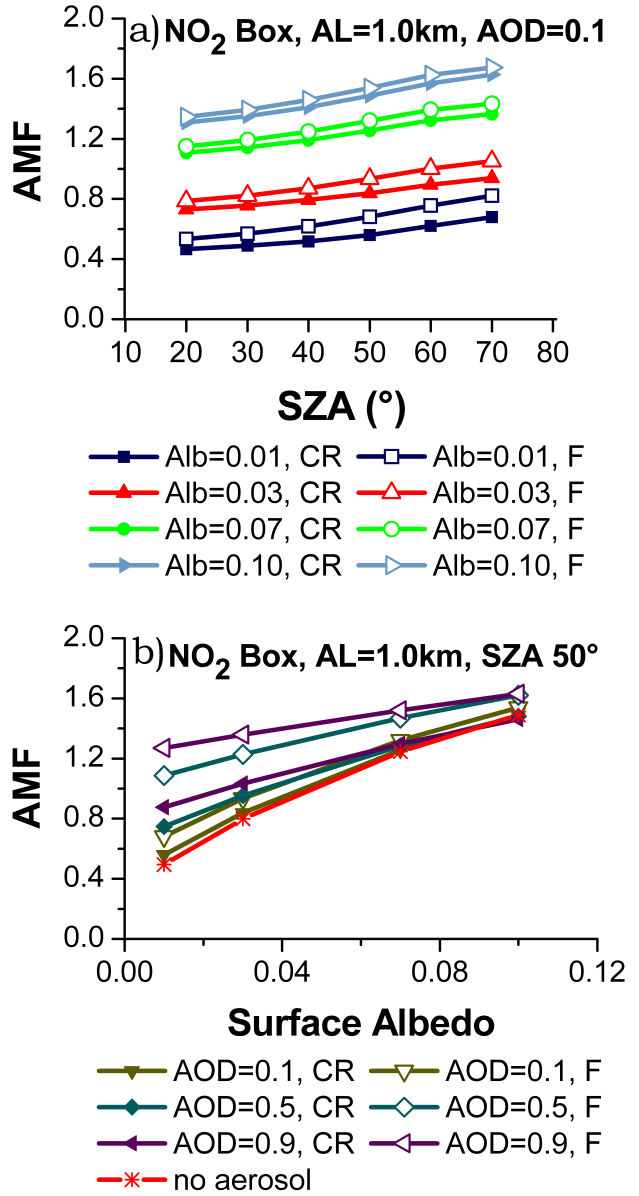


**Fig. 5.** (a) NO<sub>2</sub> airmass factors for simulations with different surface albedo (0.01 (dark blue), 0.03 (red), 0.07 (green) and 0.10 (light blue)). Scenario C (NO<sub>2</sub> and aerosol layer (AL) – 1.0 km box profile) was used with the phase functions determined for coarse (CR) and fine (F) particles (optical properties taken from Creteil/Paris AERONET station). AMFs determined at 440 nm, with  $\omega_0 = 0.93$  and AOD = 0.1. (b) AMF results for same scenario as above but for SZA = 50° and different AODs: 0.1 (green), 0.5 (blue) and 0.9 (purple), and, in addition, for the scenario without aerosol (red).

the results for different boundary layer heights, the results for NO<sub>2</sub> mixed with aerosol (Fig. 6) follow the same pattern as in the calculations performed only with the NO<sub>2</sub> layer. If a too low BL height is assumed in the retrieval, the tropospheric columns of NO<sub>2</sub> will be overestimated. However,

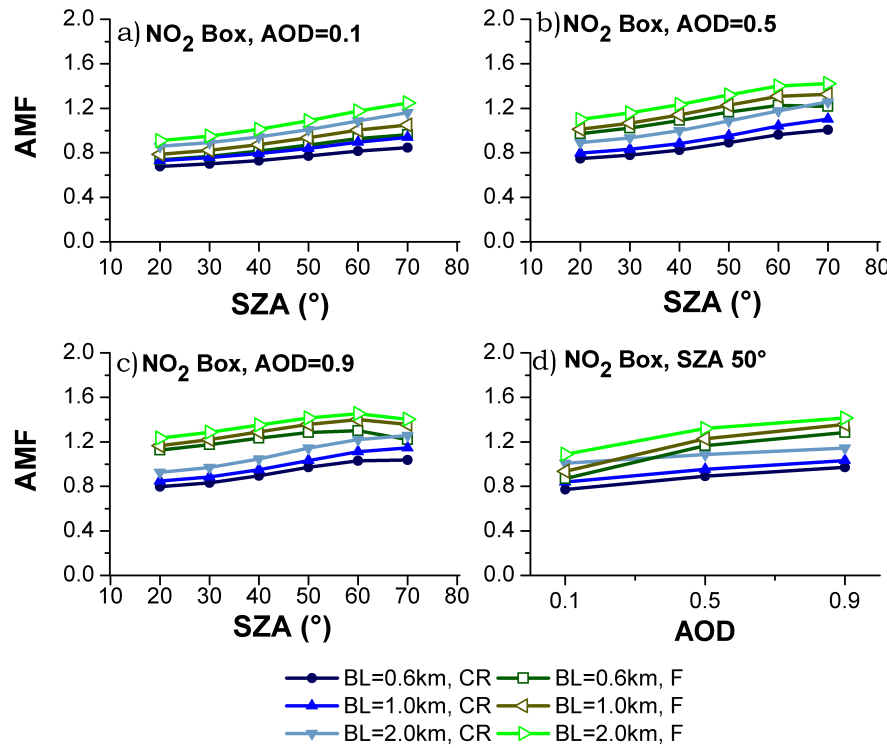


**Fig. 6.** NO<sub>2</sub> airmass factors for different boundary layer heights. Scenarios A, C and H (well mixed NO<sub>2</sub> and aerosol layers in boundary layer (BL) extending to: 0.6, 1.0 and 2.0 km, respectively) were used with the phase functions determined for coarse (CR) and fine (F) particles (optical properties taken from Creteil/Paris AERONET station). AMFs determined at 440 nm, with surface albedo = 0.03,  $\omega_0$  = 0.93 and different AODs: (a) 0.1, (b) 0.5 and (c) 0.9. AMFs results in panel (d) are presented for SZA = 50°.

the changes in the AMF are smaller in this case than for the scenarios without aerosol. The AMF increases, on average, by about 20% when the boundary layer top changes from 0.6 to 2.0 km. The largest effect was found for the simulation with coarse aerosol and optical thickness of 0.1 with 37% variation, at 440 nm. Interestingly, the effect seems to decrease with growing aerosol load. Such a variation is possibly a result of the increase in scattering (and therefore the effective albedo) which will improve the sensitivity of the satellite measurements to the lower atmosphere.

The results presented in Fig. 6 also reveal, as mentioned above, the difference in behaviour between fine and coarse particles. The AMFs resulting from the simulations with fine aerosol mixed with the trace gas are higher, i.e., at the same AOD, fine aerosol increases the sensitivity to the NO<sub>2</sub> more than coarse particles, and this difference of results increases with AOD. This is most likely related to the less pronounced forward peak in scattering on fine particles (see phase function in Fig. 3) which increases the ratio of photons scattered towards the satellite under this observation geometry and therefore improves the sensitivity.

### 3.3 Changes in extension of aerosol layer

#### Box aerosol profiles

In the previous section, NO<sub>2</sub> and aerosol had the same vertical profiles representing a situation where both are well mixed. In the following scenarios, the vertical extension of the aerosol layer was varied to 0.6 and 2.0 km (scenarios B and F, respectively) while the NO<sub>2</sub> profile was kept constant. This was done for two NO<sub>2</sub> profiles, a simple 1.0 km box profile and the more realistic urban profile as modelled by CHIMERE. Figure 7 shows the results side by side for different AODs.

As it can be observed, in general, any aerosol mixed with the trace gas tends to enhance the NO<sub>2</sub> signal, indicating that an overestimation of the NO<sub>2</sub> VC will likely occur when effects caused by aerosol presence are neglected in the retrieval. However, the magnitude of the influence does vary as it depends on the relative position of trace gas and aerosol, in particular the aerosol load above the trace gas. In addition, the size of the particles also plays a role in the calculations. As for the previous scenarios discussed above, at the same AOD, fine particles have a larger influence on the airmass factors, due to the generally higher backscattering (see Fig. 3).

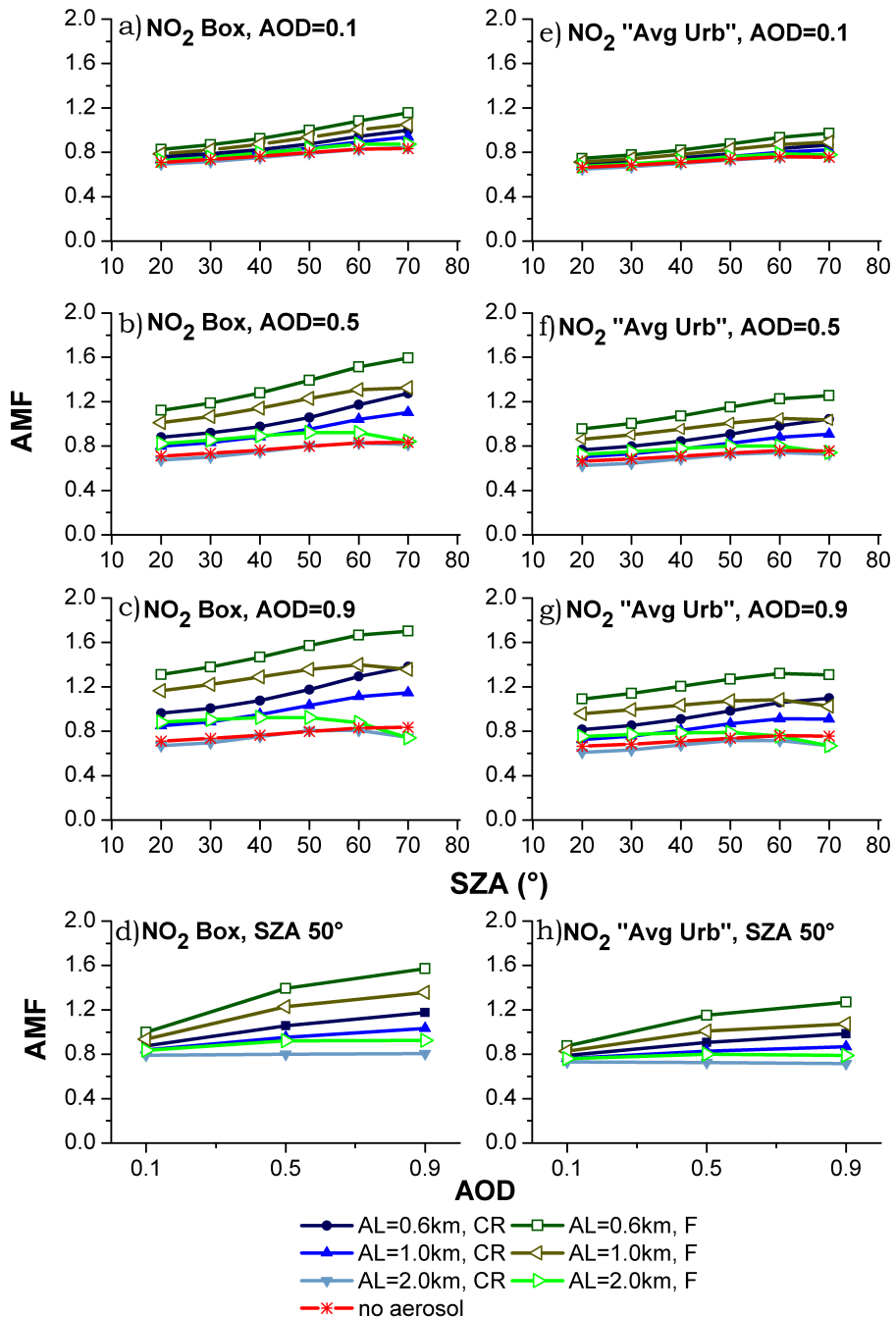


**Fig. 7.** (a)–(c) NO<sub>2</sub> airmass factors for a 1.0 km box NO<sub>2</sub> profile using no aerosol (red) and for the scenarios B, C and F (extension of aerosol layer (AL) from surface to 0.6, 1.0 and 2.0 km, respectively) calculated with the phase functions determined for coarse (CR) and fine (F) particles (optical properties taken from Creteil/Paris AERONET station). AMFs determined at 440 nm, with surface albedo = 0.03,  $\omega_0$  = 0.93 and different AODs: 0.1, 0.5 and 0.9. (e)–(g) Same as (a)–(c) for the aerosol settings but using the average of modelled urban NO<sub>2</sub> profile (“Avg Urb”). AMFs results in panel (d) and (h) are presented for SZA = 50°.

In the simulations with box profiles, the interplay between reduction and enhancement of sensitivity can explain the observed variations: if the aerosol layer is close to the surface, i.e., with its top at 600 m, below the top of the trace gas layer, the sensitivity will be enhanced due to higher reflectivity and

multiple scattering. An increase of the AMF by 11% on average is found when the top of aerosol layer lowers from 1.0 km to the 600 m and, in the case of highly polluted scenes with AOD = 0.9, the difference between the values can be as high as 25%. Compared to the simulation without aerosol, the

sensitivity can be enhanced by up to a factor of two. On the other hand, when the aerosol layer extends higher than the layer of NO<sub>2</sub>, the AMF is lower (by 5 to 45%) than in the case when both aerosol and NO<sub>2</sub> have the top layer at 1.0 km. This results from the elevated part of the layer of aerosol that acts as a shield and thereby partly cancels the enhancement of sensitivity in the lower part. Still, compared to the AMF values obtained without aerosol, the fine particles will slightly increase the NO<sub>2</sub> signal, with the exception of high solar zenith angles. In comparison, the coarse particles have smaller influence on the measurements.

The differences found in the AMFs calculated with AOD=0.1 and higher values indicate the importance of using the right AOD in the retrieval. An underestimation of the AOD will lead to an overestimation of the VC. The scenario F (aerosol layer extending to 2.0 km) is an exception to this statement as the AMF values do not vary much for different AODs.

In qualitative terms, the interpretation of the scenarios with the urban NO<sub>2</sub> profile is quite similar. However, for the latter, the AMF values are smaller as the NO<sub>2</sub> is more concentrated at the surface where the satellite sensitivity is the smallest. This is directly observed in the “no aerosol” case where the AMF decreases from 0.81 (at 440 nm and SZA=40°) to 0.70 (due to the shielding effect related to Rayleigh scattering). In addition, shielding effect of aerosols is also more pronounced for the NO<sub>2</sub> urban profile than for the 1.0 km box one, leading to an overall reduced effect of aerosols. In the case with an aerosol layer of coarse particles above the NO<sub>2</sub>, even a slight decrease in the AMF is observed. Thus, the importance of aerosols is reduced if a more realistic NO<sub>2</sub> profile is assumed.

### Measured aerosol profiles

In addition to what was described above, the model NO<sub>2</sub> profiles were also combined with aerosol profiles derived from measurements in rural areas (scenario I) and urban environments (scenarios J and K). The results are shown in Fig. 8 for calculations assuming fine and coarse particles separately. Clearly, in these particular circumstances, the aerosol effect is much smaller than before, and very close to zero in the case of typical background profiles for both the NO<sub>2</sub> and aerosol. Independently of its detailed shape, the presence of an aerosol layer tends to cover the NO<sub>2</sub> layer below thereby decreasing the sensitivity of the measurements to trace gas amounts close to the surface. Depending on the sun position and the aerosol profile, small enhancements as well as reductions in sensitivity can occur. This emphasises the point that the sensitivity of the measurements does not only depend on the vertical distribution or total load of the aerosol but the combined effect of both aerosol and NO<sub>2</sub> distribution. For coarse particles all the AMFs were smaller than for the case without aerosol, indicating that the aerosol might be pre-

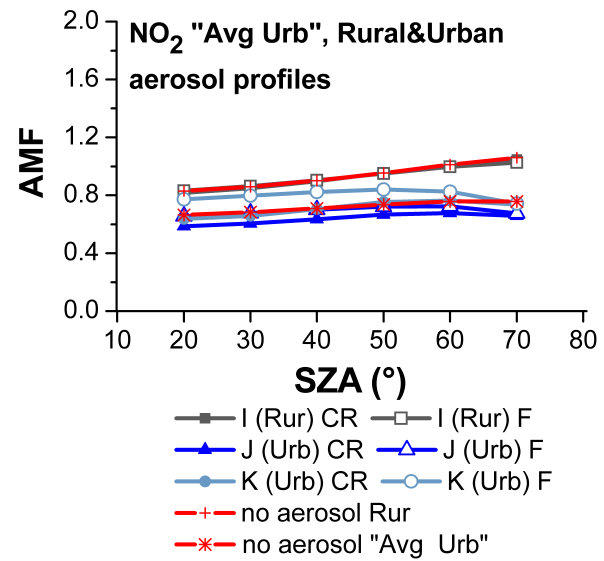


**Fig. 8.** NO<sub>2</sub> airmass factors for no aerosol (red) cases (rural – Rur – and urban – “Avg urb” – NO<sub>2</sub> profiles from CHIMERE) and for the scenarios I (background – Rur – NO<sub>2</sub> and aerosol vertical profiles), J and K (urban – Urb – NO<sub>2</sub> and aerosol vertical profiles) calculated with the phase functions determined for coarse (CR) and fine (F) particles (optical properties taken from Creteil/Paris AERONET station). AMFs determined at 440 nm, with surface albedo = 0.03,  $\omega_0$  = 0.93 (I, K) and 0.87 (J), and AOD = 0.07 (I), 0.40 (J) and 0.62 (K) (see Table 2).

venting light from reaching down lower into the NO<sub>2</sub> layer close to the surface (or back from this layer to the satellite instrument).

### 3.4 Changes in the position of the aerosol layer

#### Box aerosol profiles

The transport of dust and smoke plumes into European and certain Asian cities is not a rare event. These plumes are not only observed in the free troposphere but can, sporadically, also make a large contribution to the aerosol load measured in the boundary layer. Scenarios D, E and G (elevated aerosol layers from 0.6 to 1.0 km, from 1.0 to 2.0 km and 2.0 to 3.0 km, respectively) are simplified representations of such events with aerosol mostly being concentrated at higher altitudes. The results from these runs lead to the same conclusions as before, i.e., an aerosol layer standing above the trace gas obstructs the observation from space (see Fig. 9). A decrease of 6% to ~70% is observed when comparing the AMFs obtained for the scenario without aerosol to that with aerosol distributed from 1.0 to 2.0 km. This reduction is higher for larger aerosol load, i.e., optical thickness of 0.9. If such plumes, standing in high altitudes, are not accounted for in the retrieval process, the tropospheric VCs are underestimated. The differences of the results for the layers 1.0 to

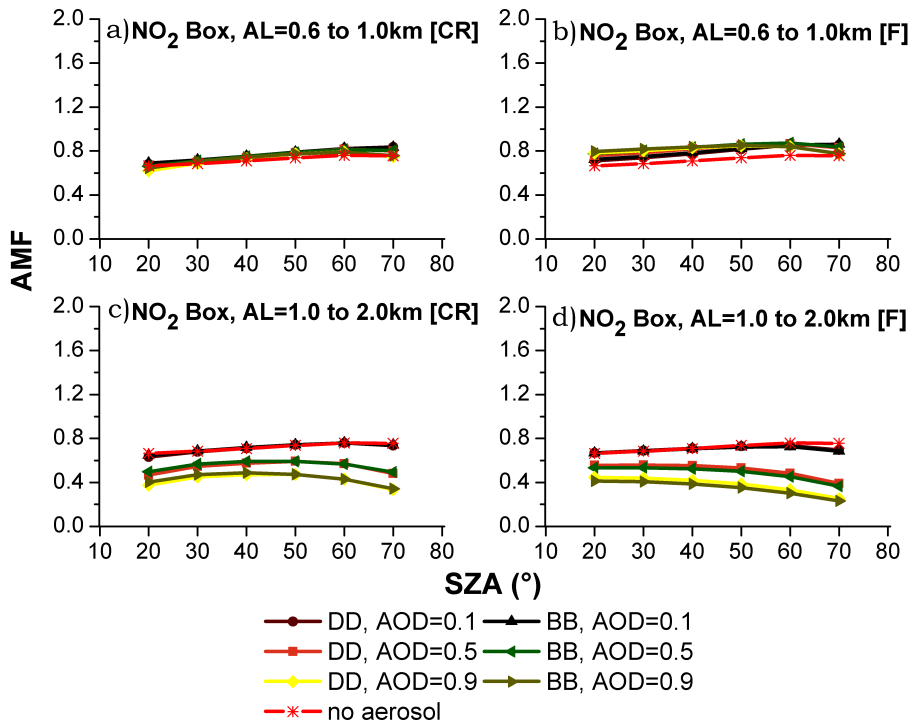


**Fig. 9.** NO<sub>2</sub> airmass factors for a 1.0 km box NO<sub>2</sub> profile using no aerosol (red) and also for scenarios D (**a**), (**b**) and E (**c**), (**d**) (elevated aerosol layers (AL) from 0.6 to 1.0 km and 1.0 to 2.0 km, respectively) calculated with the phase functions determined for (**a**), (**c**) coarse (CR) and (**b**), (**d**) fine (F) particles (optical properties taken from Amazonian Forest/Brazil and from Saudi Arabia AERONET stations, respectively for the biomass burning (BB) and desert dust (DD) cases). AMF determined at 440 nm, with surface albedo = 0.03,  $\omega_0$  = 0.93 and different AODs: 0.1, 0.5 and 0.9.

2.0 km and 2.0 to 3.0 km (not presented here) were not significant. This indicates that the height of the aerosol layer is not so relevant for the sensitivity of the measurements when there is no overlap of the trace gas and aerosol layers. Contrary to this, in the case of aerosol mixed with NO<sub>2</sub> at the top of the layer (from 0.6 to 1.0 km), it was possible to notice (Fig. 9) that the particles do not interfere much with the measurements of the trace gas (cancelling of albedo and shielding effect). In fact, a slight enhancement ( $\sim 10\%$  maximum for 440 nm) of the columns is registered only when small particles are present. It should be noted however, that this is not the case for lower SSA (see next section). In the presence of highly absorbing aerosol, the shielding effect will be dominant and a decrease of the AMF is found. Therefore, the cancelling between the two effects caused by the aerosol verified for these circumstances is naturally related to the definition of the aerosol properties.

Furthermore it is important to refer that the effect of aerosol on measurements of NO<sub>2</sub> present within a biomass burning plume will be quite different than in the case of NO<sub>2</sub> located in the boundary layer as discussed here.

### Measured aerosol profiles

In a more realistic scenario, aerosols are also present close to surface in urban areas. Therefore, profiles have been defined to include both the local plumes and those of long-range transport from biomass burning smoke or desert dust (e.g. scenarios L and P from Table 2). An example of these results is presented in Fig. 10 for desert dust layers and fire plumes measured over different cities across the globe. As it can be seen from these findings, the effect of the aerosol layers transported above polluted areas can be quite different. Once more, the reduction in the sensitivity of the measurements, when compared with the “no aerosol” case, can be negligible or as large as  $\sim 62\%$  (for scenario O). This pronounced reduction is caused by the combination of several factors: the large aerosol optical depth (AOD=1.05); its absorbing nature ( $\omega_0=0.92$ ); and the small fraction of particles that are mixed with the trace gas. This distribution of aerosol is the main difference between scenario L and O. The aerosol close to the surface present in scenario L may contribute to the cancelling of the shielding effect and therefore explain the large discrepancy between the results of the scenarios. In the case of simulations M, N and P the AMFs are not so reduced mainly because of the lower aerosol loads.

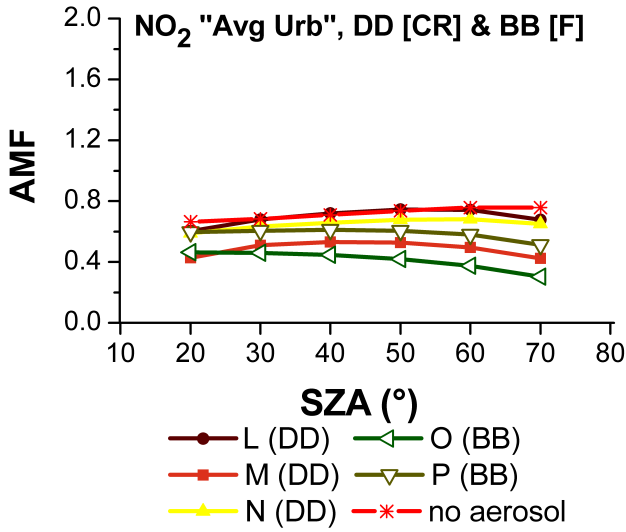


**Fig. 10.** NO<sub>2</sub> airmass factors for urban NO<sub>2</sub> profile from CHIMERE using no aerosol and also for scenarios L to P (measured aerosol profiles) calculated with the phase functions determined for desert dust (DD) coarse (CR) particles (optical properties taken from Saudi Arabia AERONET station) and for biomass burning (BB) fine (F) particles (optical properties taken from Amazonian Forest/Brazil AERONET station). AMFs determined at 440 nm, with surface albedo = 0.03, and  $\omega_0$  = 0.92 (L, O, P) and 0.93 (N) (in scenario M  $\omega_0$  varies in height from 0.80 to 0.95), and AOD = 1.05 (L, O), 0.66 (M), 0.16 (N) and 0.42 (P) (see Table 2).

For the desert dust cases, only coarse aerosol was considered in the radiative transfer calculations but both fine and coarse (not presented here) particles were used for the biomass burning situations. The difference in the AMF calculated with each of the aerosol types is in the order of 20–25% with the higher values obtained for the runs with fine aerosol.

### 3.5 Changes in single scattering albedo

As mentioned above, for all the scenarios including box profiles, the AMFs were calculated both for a single scattering albedo (SSA) of 0.93 and 1 (not presented here). However, the SSA varies in time and space. Thus, the effect of deviations in the SSA in the radiative transfer calculations was also tested by changing this parameter to 0.80 and 0.95. These results are presented for both the simulations performed with the box profiles in scenario C (Fig. 11) and scenarios J and O (Fig. 12), where the NO<sub>2</sub> modelled profiles and measured aerosol vertical distribution were considered (see Tables 1 and 2 for more details on scenarios definitions). As expected, the SSA can have a great impact on the calculation of the AMF. An increase in the absorbing properties of the aerosol (SSA decreases from 0.95 to 0.80) results in a general decrease of the AMF. While, for low aerosol load (in the scenarios with box profiles) this variation of SSA values results

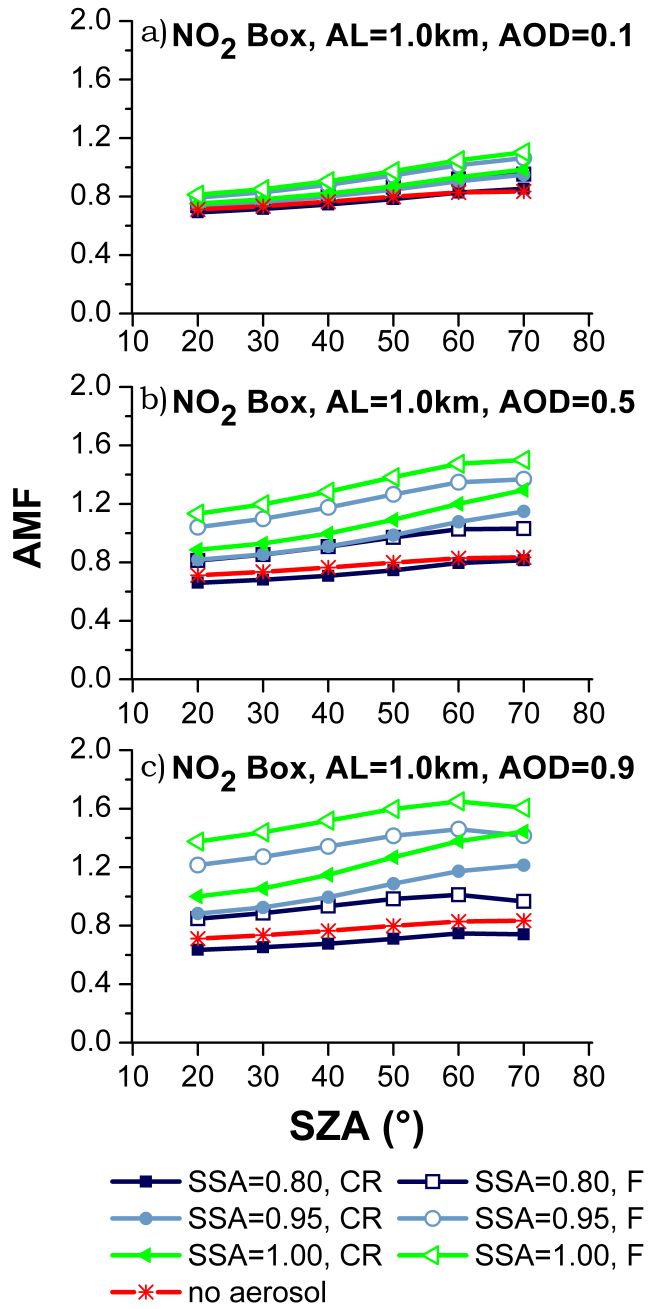


**Fig. 11.** NO<sub>2</sub> airmass factors for simulations with different single scattering albedo (SSA,  $\omega_0$  = 0.80, 0.95 and 1.00) for scenario C (NO<sub>2</sub> and aerosol layer (AL) – 1.0 km box profile), calculated with the phase functions determined for coarse (CR) and fine (F) particles (optical properties taken from Creteil/Paris AERONET station). AMFs determined at 440 nm, with surface albedo = 0.03, and different AODs: (a) 0.1, (b) 0.5 and (c) 0.9.

in a difference of the AMF on the order of 5–10%, in a more polluted atmosphere with AOD=0.9, the effect of SSA on the AMF can be as high as 77%. Still, the variation of the AMF values is not only dependent on the aerosol amount but

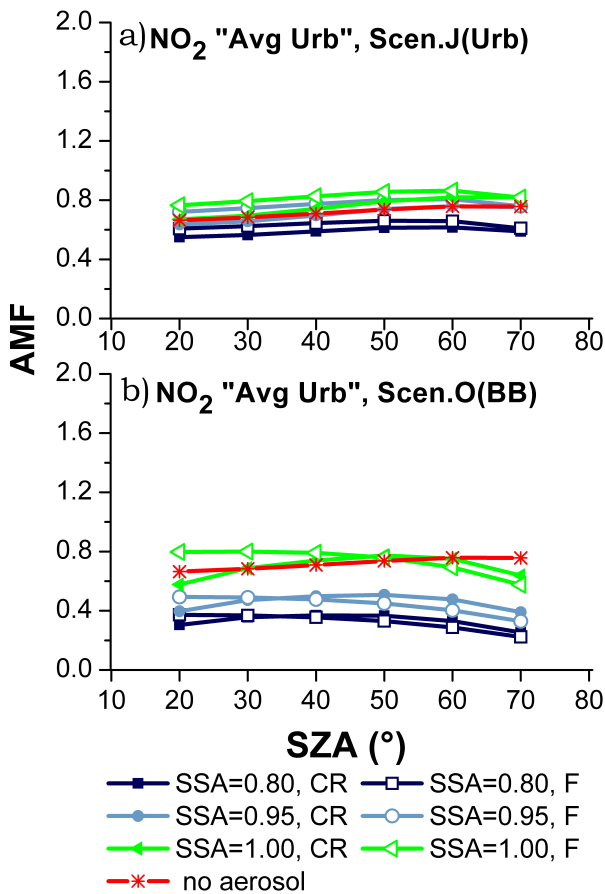


**Fig. 12.** NO<sub>2</sub> airmass factors for different single scattering albedo (SSA,  $\omega_0 = 0.80, 0.95$  and  $1.00$ ) for scenario (a) J and (b) O (urban NO<sub>2</sub> profile from CHIMERE with urban (Urb) and biomass burning (BB) aerosol, respectively) calculated with the phase functions determined for coarse (CR) and fine (F) particles (optical properties taken from Creteil/Paris and Amazonian Forest/Brazil AERONET stations for scenario J and O, respectively). AMFs determined at 440 nm, with surface albedo = 0.03, and the AOD = 0.40 (J) and 1.05 (O).

also on the profiles considered. The variation of the AMF caused by the changes in the SSA values was found to vary for different aerosol vertical distributions.

#### 4 Effect of clouds

The sensitivity analysis described here does not take into account the influence and interference of clouds on the measurements. In real data however, most measurements are affected by clouds in the satellite field of view, at least to some extent. Therefore, cloud correction algorithms are applied in the satellite retrievals to account for the effect of clouds, usually by assuming optically thick clouds and computing cloud fraction from reflectance and cloud top height from absorption of O<sub>2</sub>, O<sub>4</sub> or the amount of Raman scattering (e.g. Joiner

and Bhartia, 1995; Koelemeijer et al., 2001; Acarreta et al., 2002; Kokhanovsky et al., 2003). As the radiative effects of clouds and aerosols have large similarities, it was suggested by Boersma et al. (2004) that cloud correcting algorithms also account, even if only partly, for aerosol effects.

The presence of non-absorbing particles will increase the retrieved cloud fraction. This type of aerosol is rather comparable to thin clouds. Therefore, as a result of this similarity, if no other form of cloud is present in the field of view, the cloud correction algorithms will perform as they do on thin clouds and in fact correct for part of the aerosol effect. However, if parts of the satellite pixel are also covered by meteorological clouds, the situation changes. While the retrieved cloud fraction will again increase in the presence of aerosol, the cloud top altitude will be close to that representative for the much brighter cloud and not for that of the aerosol layer. Therefore, if the cloud is higher than the aerosol layer (which will often be the case), the cloud correction algorithm will over-compensate the shielding effect of the cloud while neglecting the enhancing effect of the low aerosol layer. As a result, cloud correction algorithms cannot compensate aerosol effects in these situations and will lead to an overestimation of any NO<sub>2</sub> below the cloud.

On the other hand, if the aerosol is absorbing, the retrieved effective cloud fraction will be too small, as the reflectance is smaller than that of a non-absorbing cloud. Also, as discussed above, the airmass factors are reduced for absorbing aerosols and this cannot be accounted for by assuming a non-absorbing cloud. An additional and more subtle difference between clouds and aerosols might be introduced by the phase function which, as mentioned before, depends on the composition and size distribution of the aerosol. This might lead to different top of atmosphere reflectance for a layer having the same optical thickness of scattering aerosol or cloud particles.

In summary, cloud retrievals can be expected to compensate aerosol effects under some conditions, but may well enhance them in other situations. As the results depend on the details of the cloud correction algorithm used, this should be investigated for each of the products in use separately.

#### 5 Conclusions

Aerosols can have a significant impact on the retrieval of tropospheric trace gases using UV/visible nadir measurements from space. In order to identify and quantify this impact, the effects of different aerosol parameters were investigated using both idealised and realistic scenarios. Overall, a large variability in the results was observed with examples of both increasing and decreasing sensitivity. The most important factors for the satellite sensitivity are not only related to aerosol assumptions, but also with the definition of surface albedo. For the latter, on average, changes of 90% of the

AMF values were registered when the surface albedo was increased from 0.01 to 0.1. This illustrates how important it is to have accurate knowledge of the surface properties. Regarding the aerosol definitions, the key factors in the determination of NO<sub>2</sub> columns were identified as the relative vertical distribution of aerosol and NO<sub>2</sub>, the AOD and the SSA. In addition, differences in the airmass factors were found when applying either coarse or fine aerosol size distribution. However, no large differences were evident when considering small variations of those main types.

Variations of the vertical extension of a well mixed boundary layer of 1.0 km containing both NO<sub>2</sub> and aerosols can result in large differences (max. 26%) of the airmass factors calculated, especially when the aerosol load is low and in low sun conditions. However, even larger effects (up to 55%) are found in the case without aerosols. The boundary layer height has strong seasonal, daily, and diurnal variations and not accounting for these changes will contribute to the inaccuracy of the calculated columns. The determined AMFs indicate that, if the boundary layer height is underestimated in the a priori assumptions, the tropospheric NO<sub>2</sub> column will be overestimated (and vice-versa).

Aerosol mixed with the trace gas, even if not on the full extension of the layer, will, by means of increased effective albedo and multiple scattering, enhance the NO<sub>2</sub> signal. In contrast, any aerosol layer that lies above the trace gas will act as a shield, decreasing the sensitivity of the measurements. If an elevated aerosol layer is not accounted for, the computed NO<sub>2</sub> columns will be too small, and this underestimation can be quite high. It is important to mention that these findings hold only for the SSA considered here (0.93), and that a dominant shielding effect is found in the event of highly absorbing aerosol mixed with the NO<sub>2</sub>. In any case, the magnitude of these effects will be determined by the relative vertical distribution of aerosol and NO<sub>2</sub>. A balance between enhancement and reduction of the signal will occur when the aerosol is both mixed with and above the NO<sub>2</sub> layer as might often be the case. As two examples, the AMF for a 1.0 km layer of NO<sub>2</sub> increases by a factor of 2 when mixed with a 600 m high from surface (Scenario B) aerosol layer of AOD 0.9, while for the case with an aerosol layer of same optical thickness between 2.0 and 3.0 km (Scenario G) the AMF is reduced by ~78%.

The absorption properties of the particles also play an important role in the retrieval of the trace gas. The largest airmass factors were always obtained for the purely scattering aerosol ( $\omega_0 = 1.0$ ). A decreasing SSA reduces the measurement sensitivity. For highly polluted scenes (AOD > 0.9) the airmass factor can increase by a factor of 1.5 and more when the single scattering albedo is modified from 0.80 to 0.95.

When more realistic vertical profiles were applied for both NO<sub>2</sub> and aerosols, a much smaller effect of aerosol was observed. Large decreases of the sensitivity of the measurements were found only for aerosol layers that are elevated or expand to higher altitudes in the atmosphere. These situa-

tions usually correspond to cases of biomass burning events or desert dust storms. For urban scenes, the changes in the airmass factors were rather small. This indicates that in these circumstances, the uncertainties introduced by neglecting the aerosol impact in the retrieval are moderate, i.e., the AMFs vary only by ~7% on average. Situations of highly polluted scenes, as those of megacities, were not fully represented here (AOD, e.g., can be much higher than 0.9). Thus, in order to allow a better understanding of the aerosol influence in the measured NO<sub>2</sub> columns, in these circumstances, further analysis is still required.

In the present study, only clear sky cases have been considered. For partially cloudy scenes the results would differ in particular if the data are corrected for cloud effects. The presence of aerosols will also impact on the retrieved cloud properties which in part can compensate the aerosol effects in the absence of real clouds. The details of the interplay between aerosol effects and cloud correction algorithms are complex and should be investigated in more detail.

The continuing use of fossil fuels and biomass burning in a changing climate will result in changes in the amounts and distribution of NO<sub>x</sub> which is one of the key precursors for tropospheric ozone. To accurately assess these changes and to efficiently allocate efforts to mitigate pollution, precise knowledge of the global tropospheric column of NO<sub>2</sub> is essential. This study shows that to improve our current knowledge of the global distributions of tropospheric NO<sub>2</sub> and its evolution, improved knowledge of the aerosol properties are required. These include the vertical profile, AOD, size distribution and also the scattering/absorption properties of the particles. Simultaneous measurements of trace gas and aerosol properties from space would be the ideal answer to solve this issue. Some instruments have the potential to retrieve both required quantities. But while this is not done, a synergistic approach can be the alternative by combining data from two instruments, e.g., using AOD from MERIS in the retrieval of NO<sub>2</sub> from SCIAMACHY (both instruments flying on the ENVISAT platform). Another promising approach is the extension of what was done in this study: a combination of satellite (e.g. MODIS, MISR, CALIPSO) and ground-based measurements (e.g., from AERONET and EARLINET networks) with model predictions, when those are available in a suitable resolution. Furthermore, not only aerosol data is required. As it was demonstrated in this analysis, the relative vertical distribution of NO<sub>2</sub> and aerosols has a large impact on the calculations. The exact shape of the NO<sub>2</sub> profile in different locations is still rather unknown. Very recently, data from ground-based measurements as, for example, those of MAX-DOAS instruments (Wagner et al., 2004) show potential to provide simultaneous measurements of trace gas and aerosol profiles in the lower troposphere. Such measurements, together with model results could be used for improved a priori data sets in the near future. Static climatological assumptions that are often used can be replaced by more up to date data that is more suitable to describe the

measurements conditions. In this way, spatial and temporal variability can be accounted for, improving the retrieval algorithm for tropospheric NO<sub>2</sub> columns.

**Acknowledgements.** This study was in part supported by the GEMS project funded by the European Commission as part of its Sixth Framework Programme and by the University of Bremen. We acknowledge the AERONET and EARLINET networks for the provision of aerosol datasets used in this study. In addition, we would like to thank Chieko Kittaka and David Winker who kindly provided CALIPSO climatologies. Finally, we would like to thank V. Rozanov, A. Rozanov and further SCIATRAN developers for the provision of the model and support throughout the study. Suggestions and comments by F. Boersma and an anonymous reviewer have helped to improve this manuscript.

Edited by: R. Martin

## References

- Acarreta, J. R., De Haan, J. F., and Stammes, P.: Cloud pressure retrieval using the O<sub>2</sub>–O<sub>2</sub> absorption band at 477 nm, *J. Geophys. Res.*, 109, D05204, doi:10.1029/2003JD003915, 2004.
- Akimoto, H.: Global air quality and pollution, *Science*, 302, 1716–1719, 2003.
- AIRPARIF: <http://www.airparif.asso.fr/>, last access: 28 February 2010.
- Amiridis, V., Balis, D. S., Kazadzis, S., Bais, A., Giannakaki, E., Papayannis, A., and Zerefos, C.: Four-year aerosol observations with a Raman lidar at Thessaloniki, Greece, in the framework of European Aerosol Research Lidar Network (EARLINET), *J. Geophys. Res.*, 110, D21203, doi:10.1029/2005JD006190, 2005.
- Ångström, A.: On the atmospheric transmission of Sun radiation and on dust in the air, *Geogr. Ann.*, 11, 156–166, 1929.
- Balis, D. S., Amiridis, V., Zerefos, C., Gerasopoulos, E., Andreae, M., Zanis, P., Kazantzidis, A., Kazadzis, S., and Papayannis, A.: Raman lidar and sunphotometric measurements of aerosol optical properties over Thessaloniki, Greece during a biomass burning episode, *Atmos. Environ.*, 37, 4529–4538, 2003.
- Beirle, S., Salzmann, M., Lawrence, M. G., and Wagner, T.: Sensitivity of satellite observations for freshly produced lightning NO<sub>x</sub>, *Atmos. Chem. Phys.*, 9, 1077–1094, 2009, <http://www.atmos-chem-phys.net/9/1077/2009/>.
- Bézy, J.-L., Delwart, S., and Rast, M.: MERIS – a new generation of ocean colour sensor onboard ENVISAT, *ESA Bull.*, 103, 48–56, 2000.
- Boersma, K. F., Eskes, H. J., and Brinksma, E. J.: Error analysis for tropospheric NO<sub>2</sub> retrieval from space, *J. Geophys. Res.*, 109, D04311, doi:10.1029/2003JD003962, 2004.
- Boersma, K. F., Eskes, H. J., Veefkind, J. P., Brinksma, E. J., van der A, R. J., Sneep, M., van den Oord, G. H. J., Levelt, P. F., Stammes, P., Gleason, J. F., and Bucsela, E. J.: Near-real time retrieval of tropospheric NO<sub>2</sub> from OMI, *Atmos. Chem. Phys.*, 7, 2103–2118, 2007, <http://www.atmos-chem-phys.net/7/2103/2007/>.
- Bovensmann, H., Burrows, J. P., Buchwitz, M., Frerick, J., Noel, S., Rozanov, V. V., Chance, K. V., and Goede, A. P. H.: SCIA-MACHY: Mission objectives and measurement modes, *J. Atmos. Sci.*, 56(2), 127–150, doi:10.1175/1520-0469, 1999.
- Burrows, J. P., Holzle, E., Goede, A. P. H., Visser, H., and Fricke, W.: SCIAMACHY – Scanning Imaging Absorption Spectrometer for Atmospheric Chartography, *Acta Astronaut.*, 35, 445–451, 1995.
- Burrows, J. P., Weber, M., Buchwitz, M., Rozanov, V., Ladstätter-Weißenmayer, A., Richter, A., DeBeek, R., Hoogen, R., Bramstedt, K., Eichmann, K.-U., Eisinger, M., and Perner, D.: The Global Ozone Monitoring Experiment (GOME): Mission concept and first scientific results, *J. Atmos. Sci.*, 56(2), 151–175, doi:10.1175/1520-0469, 1999.
- Callies, J., Corpaccioli, E., Eisinger, M., Hahne, A., and Lefebvre, A.: GOME-2 – Metop's second generation sensor for operational ozone monitoring, *ESA Bull.*, 102, 28–36, 2000.
- Chang, D., Song, Y., and Liu, B.: Visibility trends in six megacities in China 1973–2007, *Atmos. Res.*, 94, 161–167, 2009.
- Chazette, P., Randriamiarisoa, H., Sanak, J., Couvert, P., and Flamant, C.: Optical properties of urban aerosol from airborne and ground-based in situ measurements performed during the Etude et Simulation de la Qualité de l'air en Ile de France (ESQUIF) program, *J. Geophys. Res.*, 110, D02206, doi:10.1029/2004JD004810, 2005.
- Chen, D., Zhou, B., Beirle, S., Chen, L. M., and Wagner, T.: Tropospheric NO<sub>2</sub> column densities deduced from zenith-sky DOAS measurements in Shanghai, China, and their application to satellite validation, *Atmos. Chem. Phys.*, 9, 3641–3662, 2009, <http://www.atmos-chem-phys.net/9/3641/2009/>.
- Diner, D. J., Beckert, J. C., Reilly, T. H., Bruegge, C. J., Conel, J. E., Kahn, R. A., Martonchik, J. V., Ackerman, T. P., Davies, R., Gerstl, S. A. W., Gordon, H. R., Muller, J.-P., Myneni, R. B., Sellers, P. J., Pinty, B., and Verstraete, M. M.: Multi-angle Imaging Spectroradiometer (MISR) instrument description and experiment overview, *IEEE Trans. Geosci. Remote*, 36, 1072–1087, 1998.
- Dubovik, O., Holben, B., Eck, T. F., Smirnov, A., Kaufman, Y. F., King, M. D., Tanré, D., and Slutsker, I.: Variability of absorption and optical properties of key aerosol types observed in worldwide locations, *J. Atmos. Sci.*, 59, 590–608, 2002.
- Fu, T.-M., Jacob, D. J., Palmer, P. I., Chance, K., Wang, Y. X., Barletta, B., Blake, D. R., Stanton, J. C., and Pilling, M. J.: Space-based formaldehyde measurements as constraints on volatile organic compound emissions in east and south Asia and implications for ozone, *J. Geophys. Res.*, 112, D06312, doi:10.1029/2006JD007853, 2007.
- Gloudemans, A. M. S., Schrijver, H., Hasekamp, O. P., and Aben, I.: Error analysis for CO and CH<sub>4</sub> total column retrievals from SCIAMACHY 2.3 μm spectra, *Atmos. Chem. Phys.*, 8, 3999–4017, 2008, <http://www.atmos-chem-phys.net/8/3999/2008/>.
- Heckel, A., Kim, S.-W., Frost, G. J., Richter, A., Trainer, M., and Burrows, J. P.: Influence of under-sampling in a priori data on tropospheric NO<sub>2</sub> satellite retrievals, *Atmos. Meas. Tech. Discuss.*, to be submitted, 2010.
- Hild, L., Richter, A., Rozanov, V., and Burrows, J. P.: Air mass factor calculations for GOME measurements of lightning-produced NO<sub>2</sub>, *Adv. Space Res.*, 29(11), 1685–1690, 2002.
- Holben, B. N., Eck, T. F., Slutsker, I., Tanré, D., Buis, J. P., Setzer, A., Vermote, E., Reagan, J. A., Kaufman, Y., Nakajima, T.,

- Lavenu, F., Jankowiak, I., and Smirnov, A.: AERONET – A federated instrument network and data archive for aerosol characterization, *Remote Sens. Environ.*, 66, 1–16, 1998.
- Honoré, C., Rouil, L., Vautard, R., Beekmann, M., Bessagnet, B., Dufour, A., Elichegaray, C., Flaud, J.-M., Malherbe, L., Meleux, F., Menut, L., Martin, D., Peuch, A., Peuch, V. H., and Poisson, N.: Predictability of European air quality: The assessment of three years of operational forecasts and analyses by the PREV'AIR system, *J. Geophys. Res.*, 113, D04301, doi:10.1029/2007JD008761, 2008.
- Hu, R.-M., Martin, R. V., and Fairlie, T. D.: Global retrieval of columnar aerosol single scattering albedo from spacebased observations, *J. Geophys. Res.*, 112, D02204, doi:10.1029/2005JD006832, 2007.
- IPCC: Climate Change 2007: The Physical Science Basis. Contribution of Working Group I to the Fourth Assessment Report of the Intergovernmental Panel on Climate Change, edited by: Solomon, S., Qin, D., Manning, M., Chen, Z., Marquis, M., Averyt, K. B., Tignor, M., and Miller, H. L., Cambridge University Press, Cambridge, United Kingdom and New York, NY, USA, 2007.
- Joiner, J. and Bhartia, P. K.: The determination of cloud pressures from rotational raman-scattering in satellite backscatter ultraviolet measurements, *J. Geophys. Res.*, 100(D11), 23019–23026, 1995.
- King, M. D., Kaufman, Y. J., Menzel, W. P., and Tanré, D.: Remote sensing of cloud, aerosol, and water vapor properties from the Moderate Resolution Imaging Spectrometer (MODIS), *IEEE Trans. Geosci. Remote*, 30(1), 2–27, 1992.
- Koelemeijer, R. B. A., Stammes, P., Hovenier, J. W., and de Haan, J. F.: A fast method for retrieval of cloud parameters using oxygen A band measurements from the Global Ozone Monitoring Experiment, *J. Geophys. Res.*, 106, 3475–3490, 2001.
- Kokhanovsky, A. A., Rozanov, V. V., Zege, E. P., Bovensmann, H., and Burrows, J. P.: A semianalytical cloud retrieval algorithm using backscattered radiation in 0.4–2.4 μm spectral region, *J. Geophys. Res.*, 108(D1), 4008, doi:10.1029/2001JD001543, 2003.
- Kokhanovsky, A. A. and Rozanov, V. V.: Retrieval of NO<sub>2</sub> vertical columns under cloudy conditions: A sensitivity study based on SCIATRAN calculations, *Atmos. Res.*, 93, 695–699, 2009.
- Krueger, A., Walter, L., Bhartia, P. K., Schnetzer, C., Krotkov, N., Sprod, I., and Bluth, G.: Volcanic sulfur dioxide measurements from the total ozone mapping spectrometer instruments, *J. Geophys. Res.*, 100(D7), 14057–14076, 1995.
- Labonne, M., Bréon, F.-M., and Chevallier, F.: Injection height of biomass burning aerosols as seen from a spaceborne lidar, *Geophys. Res. Lett.*, 34, L11806, doi:10.1029/2007GL029311, 2007.
- Lee, C., Martin, R. V., van Donkelaar, A., O'Byrne, G., Krotkov, N., Richter, A., Huey, G., and Holloways, J. S.: Retrieval of vertical columns of sulfur dioxide from SCIAMACHY and OMI: Air mass factor algorithm development and validation, *J. Geophys. Res.*, 114, D22303, doi:10.1029/2009JD012123, 2009.
- Leue, C., Wenig, M., Wagner, T., Klimm, O., Platt, U., and Jähne, B.: Quantitative analysis of emissions from Global Ozone Monitoring Experiment satellite image sequences, *J. Geophys. Res.*, 106(D6), 5493–5505, 2001.
- Levelt, P. F., van den Oord, G. H. J., Dobber, M. R., Mälkki, A., Visser, H., de Vries, J., Stammes, P., Lundell, J. O. V., and Saari, H.: The Ozone Monitoring Instrument, *IEEE Trans. Geosci.* Remote, 44(5), 1093–1101, doi:10.1109/TGRS.2006.872333, 2006.
- Martin, R. V., Chance, K., Jacob, D. J., Kurosu, T. P., Spurr, R. J. D., Bucsela, E., Gleason, J. F., Palmer, P. I., Bey, I., Fiore, A. M., Li, Q., Yantosca, R. M., and Koelemeijer, R. B. A.: An improved retrieval of tropospheric nitrogen dioxide from GOME, *J. Geophys. Res.*, 107(D20), 4437, doi:10.1029/2001JD001027, 2002.
- Martin, R. V., Jacob, D. J., Chance, K., Kurosu, T. P., Palmer, P. I., and Evans, M. J.: Global inventory of nitrogen oxide emissions constrained by space-based observations of NO<sub>2</sub> columns, *J. Geophys. Res.*, 108(D17), 4537, doi:10.1029/2003JD003453, 2003.
- Mattis, I., Ansmann, A., Müller, D., Wandinger, U., and Althausen, D.: Dual-wavelength Raman lidar observations of the extinction-to-backscatter ratio of Saharan dust, *Geophys. Res. Lett.*, 29(9), 1306, doi:10.1029/2002GL014721, 2002.
- Mattis, I., Ansmann, A., Müller, D., Wandinger, U., and Althausen, D.: Multiyear aerosol observations with dual-wavelength Raman lidar in the framework of EARLINET, *J. Geophys. Res.*, 109, D13203, doi:10.1029/2004JD004600, 2004.
- Mishchenko FORTRAN codes: <http://www.giss.nasa.gov/staff/m mishchenko/brf/>, last access: October 2009.
- Müller, D., Mattis, I., Wandinger, U., Ansmann, A., Althausen, D., Dubovik, O., Eckhardt, S., and Stohl, A.: Saharan dust over a central European EARLINET-AERONET site: Combined observations with Raman lidar and Sun photometer, *J. Geophys. Res.*, 108(D12), 4345, doi:10.1029/2002JD002918, 2003.
- Müller, D., Mattis, I., Wandinger, U., Ansmann, A., Althausen, D., and Stohl, A.: Raman lidar observations of aged Siberian and Canadian forest fire smoke in the free troposphere over Germany in 2003: Microphysical particle characterization, *J. Geophys. Res.*, 110, D17201, doi:10.1029/2004JD005756, 2005.
- Murayama, T., Sugimoto, N., Uno, I., Kinoshita, K., Aoki, K., Hagiwara, N., Liu, Z., Matsui, I., Sakai, T., Shibata, T., Arao, K., Sohn, B.-J., Won, J.-G., Yoon, S.-Y., Li, T., Zhou, J., Hu, H., Abo, M., Iokibe, K., Koga, R., and Iwasaka, Y.: Ground-based network observation of Asian dust events of April 1998 in East Asia, *J. Geophys. Res.*, 106(D16), 18345–18359, 2001.
- Murayama, T., Masonis, S. J., Redemann, J., Anderson, T. L., Schmid, B., Livingston, J. M., Russell, P. B., Huebert, B., Howell, S. G., McNaughton, C. S., Clarke, A., Abo, M., Shimizu, A., Sugimoto, N., Yabuki, M., Kuze, H., Fukagawa, S., Maxwell-Meier, K., Weber, R. J., Orsini, D. A., Blomquist, B., Bandy, A., and Thornton, D.: An intercomparison of lidar-derived aerosol optical properties with airborne measurements near Tokyo during ACE-Asia, *J. Geophys. Res.*, 108(D23), 8651, doi:10.1029/2002JD003259, 2003.
- Nüß, J. H.: Verbes serungen des troposphärischen NO<sub>2</sub>-Retrievals aus GOME- und SCIAMACHY-Daten, Ph.D. Thesis, Bremen University, Bremen, 2005.
- Pérez, C., Nickovic, S., Baldasano, J. M., Sicard, M., Rocadenbosch, F., and Cachorro, V. E.: A long Saharan dust event over the western Mediterranean: lidar, sunphotometer observations, and regional dust modeling, *J. Geophys. Res.*, 111, D15214, doi:10.1029/2005JD006579, 2006.
- Platt, U. and Stutz, J.: Differential Optical Absorption Spectroscopy: Principles and Applications, in: Physics of Earth and Space Environments, Springer, Berlin, 2008.

- Richter, A. and Burrows, J. P.: Tropospheric NO<sub>2</sub> from GOME measurements, *Adv. Space Res.*, 29(11), 1673–1683, 2002.
- Richter, A., Burrows, J. P., Nüß, H., Granier, C., and Niemeier, U.: Increase in tropospheric nitrogen dioxide over China observed from space, *Nature*, 437, 129–132, 2005.
- Rozanov, A., Rozanov, V., Buchwitz, M., Kokhanovsky, A., and Burrows, J. P.: SCIATRAN 2.0 – A new radiative transfer model for geophysical applications in the 175–2400 nm spectral region, *Adv. Space Res.*, 36(5), 1015–1019, doi:10.1016/j.asr.2005.03.012, 2005.
- Rozanov, V. V. and Rozanov, A. V.: Differential optical absorption spectroscopy (DOAS) and air mass factor concept for a multiply scattering vertically inhomogeneous medium: theoretical consideration, *Atmos. Meas. Tech. Discuss.*, 3, 697–784, 2010, <http://www.atmos-meas-tech-discuss.net/3/697/2010/>.
- Schmidt, H., Derognat, C., Vautard, R., and Beekmann, M.: A comparison of simulated and observed ozone mixing ratios for summer of 1998 in western Europe, *Atmos. Environ.*, 35, 6277–6297, 2001.
- Seinfeld, J. H. and Pandis, S. N.: Atmospheric Chemistry and Physics: From Air Pollution to Climate Change, John Wiley & Sons, New York, 1998.
- Solomon, S., Schmeltekopf, A. L., and Sanders, R. W.: On the interpretation of zenith sky absorption measurements, *J. Geophys. Res.*, 92(D7), 8311–8319, 1987.
- Solomon, S., Portmann, W., Sanders, R. W., Daniel, J. S., Madson, W., Bartram, B., and Dutton, E. G.: On the role of nitrogen dioxide in the absorption of solar radiation, *J. Geophys. Res.*, 104(D10), 12047–12058, 1999.
- Thomas, W., Erbertseder, T., Ruppert, T., van Roozendael, M., Verdebout, J., Balis, D., Meleti C., and Zerefos, C.: On the retrieval of volcanic sulfur dioxide emissions from GOME backscatter measurements, *J. Atmos. Chem.*, 50, 295–320, doi:10.1007/s10874-005-5544-1, 2005.
- Vasilkov, A. P., Joiner, J., Oreopoulos, L., Gleason, J. F., Veefkind, P., Bucsela, E., Celarier, E. A., Spurr, R. J. D., and Platnick, S.: Impact of tropospheric nitrogen dioxide on the regional radiation budget, *Atmos. Chem. Phys.*, 9, 6389–6400, 2009, <http://www.atmos-chem-phys.net/9/6389/2009/>.
- Wang, K., Dickinson, R. E., and Liang, S.: Clear sky visibility has decreased over land globally from 1973 to 2007, *Science*, 323, 1468–1470, 2009.
- Wang, P., Richter, A., Bruns, M., Rozanov, V. V., Burrows, J. P., Heue, K.-P., Wagner, T., Pundt, I., and Platt, U.: Measurements of tropospheric NO<sub>2</sub> with an airborne multi-axis DOAS instrument, *Atmos. Chem. Phys.*, 5, 337–343, 2005, <http://www.atmos-chem-phys.net/5/337/2005/>.
- Wagner, T., Dix, B., von Friedeburg, C., Frieß, U., Sanghavi, S., Sinreich, R., and Platt, U.: MAX-DOAS O<sub>4</sub> measurements: A new technique to derive information on atmospheric aerosols – Principles and information content, *J. Geophys. Res.*, 109, D22205, doi:10.1029/2004JD004904, 2004.
- Wagner, T., Burrows, J. P., Deutschmann, T., Dix, B., von Friedeburg, C., Frieß, U., Hendrick, F., Heue, K.-P., Irie, H., Iwabuchi, H., Kanaya, Y., Keller, J., McLinden, C. A., Oetjen, H., Palazzi, E., Petritoli, A., Platt, U., Postylyakov, O., Pukite, J., Richter, A., van Roozendael, M., Rozanov, A., Rozanov, V., Sinreich, R., Sanghavi, S., and Witrock, F.: Comparison of box-airmass-factors and radiances for Multiple-Axis Differential Optical Absorption Spectroscopy (MAX-DOAS) geometries calculated from different UV/visible radiative transfer models, *Atmos. Chem. Phys.*, 7, 1809–1833, 2007, <http://www.atmos-chem-phys.net/7/1809/2007/>.
- Winker, D. M., Pelon, J. R., and McCormick, M. P.: The CALIPSO mission: Spaceborne lidar for observation of aerosols and clouds, in: Proceedings of the Lidar Remote Sensing for Industry and Environment Monitoring III Conference, Hangzhou, China, 24 October 2002, 4893, 1–11, 2003.
- Zhou, J., Yu, G., Jin, C., Qi, F., Liu, D., Hu, H., Gong, Z., Shi, G., Nakajima, T., and Takamura, T.: Lidar observations of Asian dust over Hefei, China, in spring 2000, *J. Geophys. Res.*, 107(D15), 4252, doi:10.1029/2001JD000802, 2002.